AIP | The Journal of Chemical Physics

The spectroscopic and photophysical effects of the position of methyl substitution. II. 2methylpyrimidine

Ralph E. Bandy, Aaron W. Garrett, H. D. Lee, and Timothy S. Zwier

Citation: The Journal of Chemical Physics **96**, 1667 (1992); doi: 10.1063/1.462121
View online: http://dx.doi.org/10.1063/1.462121
View Table of Contents: http://scitation.aip.org/content/aip/journal/jcp/96/3?ver=pdfcov
Published by the AIP Publishing

The spectroscopic and photophysical effects of the position of methyl substitution. II. 2-methylpyrimidine

Ralph E. Bandy, Aaron W. Garrett, H. D. Lee, and Timothy S. Zwier[a),b)]
Department of Chemistry, Purdue University, West Lafayette, Indiana 47907-1393

(Received 30 August 1991; accepted 17 October 1991)

Laser-induced fluorescence excitation and dispersed fluorescence spectra of the first n–π^* transition of jet-cooled 2-methylpyrimidine have been recorded and analyzed. This work extends our earlier study of the spectroscopic and photophysical effects of methyl substitution in 4- and 5-methylpyrimidine. An unusual Fermi resonance involving the $6a_0^n$ progression forms the focus of the present study. The $6a_0^1$ vibronic transition is observed to be split into a triad of transitions. Dispersed fluorescence spectra are used to identify the dark background state responsible for the Fermi resonance coupling as the $16b^1(3a_2'')$ vibration/internal rotation combination level. This level is selectively coupled by symmetry constraints to $6a^1(0a_1')$, leaving the $6a^1(1e'')$ level unperturbed. The positions and intensities of the triad of peaks in the excitation spectrum allow a quantitative determination of the $6a^1(0a_1')\leftrightarrow 16b^1(3a_2'')$ coupling matrix element of $V=4.1$ cm^{-1}. This vibration/internal rotation Fermi resonance is thus typical of the new types of routes to vibrational state mixing which are opened by methyl substitution. Higher members of the $6a_0^n$ progression are also involved in Fermi resonance mixing. However, in addition, these levels experience weaker, less state-specific coupling to a bath of same-symmetry states at that energy. The excitation spectrum provides an estimate of the average coupling matrix element of this second tier coupling of ~ 1 cm^{-1}.

I. INTRODUCTION

The hindered internal rotation of a methyl group is increasingly becoming recognized as a sensitive probe of its local steric and electronic environment. Dramatic changes in the barrier height have been observed with changing position of methyl substitution, electronic state, and charge.[1-6] In an effort to better understand such effects, we have recently reported on spectroscopic studies of 4- and 5-methylpyrimidine shown below (hereafter referred to as 4-mp and 5-mp, respectively).[6] Substitution in the symmetric 5 position renders the methyl group a nearly free rotor ($V_6 \sim 4$ cm^{-1}) in both the S_0 and S_1 states. However, asymmetric substitution in the 4 position produces a threefold barrier, while simultaneously raising the barrier to 95 cm^{-1} in the S_0 state and over 700 cm^{-1} in the S_1 state.

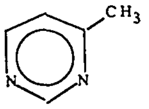

4-mp

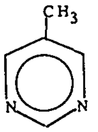

5-mp

2-mp

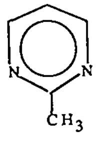

The present paper extends our study of methylpyrimidines to include 2-methylpyrimidine (2-mp) using the same techniques of laser-induced fluorescence and dispersed fluorescence in a supersonic free jet. We will see that the spectroscopy of 2-mp has many similarities to that of 5-mp. Both compounds are of G_{12} molecular symmetry[7] with a V_6 potential for the barrier to internal rotation. We will see that the internal rotor barrier in 2-mp, like that in 5-mp, is exceedingly small[8] (2 cm^{-1}) in both S_0 and S_1 states.

The comparison of 2-, 4-, and 5-mp also affords an interesting look at the extent and mechanism of the enhancement of vibrational state mixing which accompanies methyl substitution. The fluorescence excitation and dispersed fluorescence spectra of 2-mp provide a particularly clear example of vibration-internal rotation coupling at the $6a^n$ levels. This coupling is manifested as a Fermi resonance in the fluorescence excitation spectrum. The dispersed fluorescence spectra have been used to clearly identify the vibration/internal rotation band responsible for the mixing. The positions and intensities of the coupled levels allow the determination of the degree of mixing of the Fermi levels and an absolute measure of the vibration/internal rotation coupling matrix element.

II. EXPERIMENT

The apparatus used in this study is described in detail elsewhere.[9] 2-mp is cooled in a supersonic expansion by passing helium (3 bar) over the room temperature liquid and expanding the mixture through a pulsed valve (General Valve, 0.5 mm diam.) into the vacuum chamber. The expansion is crossed 1 cm downstream with the doubled output of an excimer pumped dye laser using either rhodamine 640 or sulforhodamine 640 dye. Fluorescence excitation spectra are recorded by collecting the total fluorescence through a 370 nm cut-off filter using a UV-sensitive photomultiplier tube and gated integration. With the use of an intracavity etalon, a wavelength resolution of 0.08 cm^{-1} in the ultraviolet is obtained for rotational band contour scans. Dispersed fluorescence (DFL) spectra are recorded using a 3/4-m mono-

---

[a)] Author to whom correspondence should be addressed.
[b)] Alfred P. Sloan Research Fellow.

chromator. Resolutions ranging from 30 to 80 $\mathrm{cm^{-1}}$ full width at half-maximum (FWHM) were obtained depending on the signal intensity. The low fluorescence quantum yield of the S_1 state of 2-mp requires the use of gated photon counting in the DFL scans (Stanford SR400). Typical signal levels in dispersed fluorescence are one photon/five laser shots.

Infrared spectra of the neat liquid of 2-mp were recorded on a Perkin Elmer 1800 Fourier transform infrared spectrometer at 2 $\mathrm{cm^{-1}}$ resolution using polyethylene as sample container to allow absorptions down to 200 $\mathrm{cm^{-1}}$ to be observed.

2-Methylpyrimidine was prepared from *N*-acetyl-1,3-diaminopropane according to the published procedure.[10] The *N*-acetyl-1,3-diaminopropane used as starting material was prepared by adding, dropwise, ethylacetate (10 mL, 0.1 mol) to 1,3-diaminopropane (100 mL, 1.2 mol) and heating the mixture at 90 °C for 16 h. After cooling, the excess 1,3-diaminopropane was removed at reduced pressure (0.05 Torr) at 40 °C to give an oily residue, identified as *N*-acetyl-1,3-diaminopropane (11.0 g, 95% yield). The residue was dissolved in 150 mL of *o*-xylene and the solution heated under reflux (170 °C) for two days to provide the cyclic 2-methyl-1,4,5,6-tetrahydropyrimidine. This product was dehydrogenated subsequently by passing it upon elution with nitrogen through a 350 °C Vycor tube containing Pd/Al_2O_3 pellets as catalyst. The crude 2-methylpyrimidine product was purified by double distillation to obtain 5.47 g product (58% overall yield) with bp 130–132 °C. GC (DB-WAX) analysis indicated > 98% chemical purity. ^{1}H nuclear magnetic resonance (NMR) ($CDCl_3$) δ 8.68 (*d*, 2H), 7.14 (*t*, 1H), and 2.76 (*s*, 3H). *MS*:*EI*, *m*/*e* 94 (*m*), 67 (m-C_2H_3); CI (isobutane), *m*/*e* 95 ($m+\mathrm{H}$).

III. RESULTS AND DISCUSSION

A. Fluorescence excitation and dispersed fluorescence spectra

Figure 1 presents the first 1500 $\mathrm{cm^{-1}}$ of the S_0–S_1 n–π^* fluoresence excitation spectrum of 2-mp. Table I summarizes the observed positions and relative intensities of the main transitions. The origin is observed at 30 467 $\mathrm{cm^{-1}}$, 1414 $\mathrm{cm^{-1}}$ red shifted from the S_0–S_1 origin transition in pyrimidine.[11] The close correspondence of the fluorescence excitation spectra of 2-mp with those of pyrimidine and 5-mp is highlighted in a comparison of Fig. 1 (2-mp) with Figs. 2(a) (pyrimidine) and 2(b) (5-mp). All three spectra are very similar in having virtually no activity before $6a_0^1$. This is the region where we would expect to see some intensity in internal rotor transitions if significant changes occur either in the height or phase angle of the internal rotor barrier upon electronic excitation. The almost total lack of intensity in this region is thus the first indication that the barrier to internal rotation in the excited state is very low, just as it is in the ground state ($V_6'' = 2$ $\mathrm{cm^{-1}}$).[8] Further evidence to support this contention is present in the high resolution etalon scan of the origin transition (Fig. 3). The different nuclear spin symmetries of the $0a_1'$ and $1e''$ ground state internal rotor levels hinders cooling between the lowest two internal rotor levels.[5,6] Thus if there were any appreciable change to the barrier upon going from S_0 to S_1, we would expect to see a splitting between the $0_0^0(0a_1'$–$0a_1')$ and the $0_0^0(1e''$–$1e'')$ transitions. The single Q branch present in the spectrum indicates that we are unable at our resolution to resolve the $0a_1/1e$ splitting, providing strong evidence that the barrier to methyl internal rotation in 2-mp remains virtually unchanged upon electronic excitation.

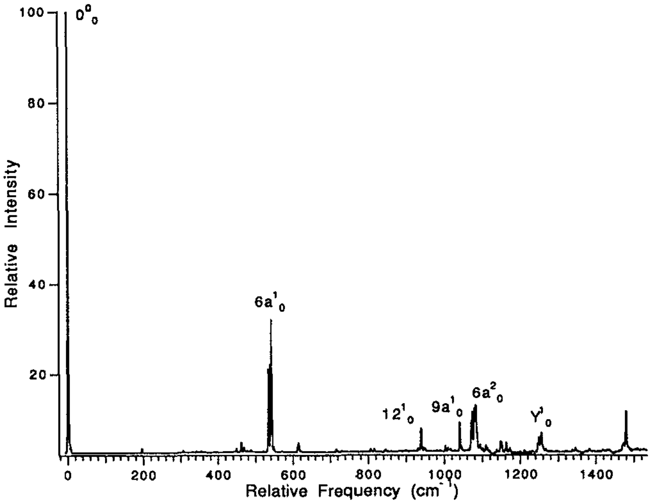

FIG. 1. Fluoresence excitation spectrum of the first 1500 $\mathrm{cm^{-1}}$ of the $S_1 \leftarrow S_0$ transition of jet-cooled 2-methylpyrimidine. The absolute frequency of the origin is 30 467 $\mathrm{cm^{-1}}$.

The dispersed fluorescence spectrum from the zero point S_1 level is shown in Fig. 4. Quantitative positions and intensities are given in Table II. Infrared spectra of the neat liquid were also recorded in order to obtain ground state vibrational frequencies to aid in the assignment of the dispersed fluorescence spectra. The observed infrared transi-

TABLE I. Frequencies, relative intensities, and assignments of transitions in the S_0–S_1 excitation spectrum of 2-methylpyrimidine.

Frequency ($\mathrm{cm^{-1}}$)	Relative intensity	Assignments
0[a]	100	0_0^0
197	4	$0_0^0(6a_1)$
462	5	...
534.5[b]	21	$6a_0^1 0a_1 16b\,^13a_2$
540	22	$6a_0^1 1e$
543[b]	32	$6a_0^1 0a_1 16b\,^13a_2$
615	5	...
940	8	12_0^1
1003	4	...
1040	10	$9a_0^1$
1082	13	$6a_0^2$
1147	5	...
1163	5	...
1255	7	...
1479	12	$6a_0^1 12_0^1$ (?)

[a] All frequencies are relative to the origin transition (0_0^0) which occurs at an absolute frequency of 30 467 $\mathrm{cm^{-1}}$.

[b] The levels at 534.5 and 543 are in Fermi resonance with one another. See the text for further discussion.

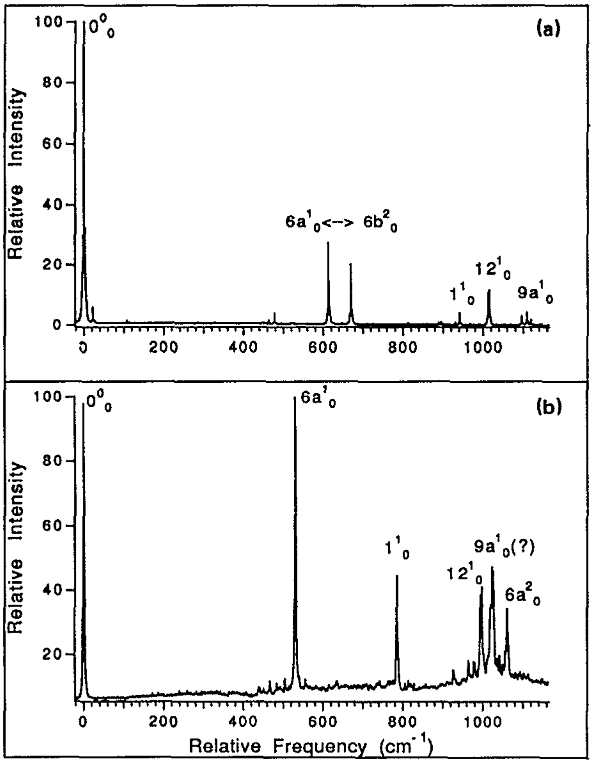

FIG. 2. Fluoresence excitation spectra of the first 1100 cm^{-1} of the $S_1 \leftarrow S_0$ transition of (a) pyrimidine and (b) 5-methylpyrimidine cooled in a supersonic expansion. The double arrow in (a) denotes the Fermi resonance between $6a_0^1$ and $6b_0^2$.

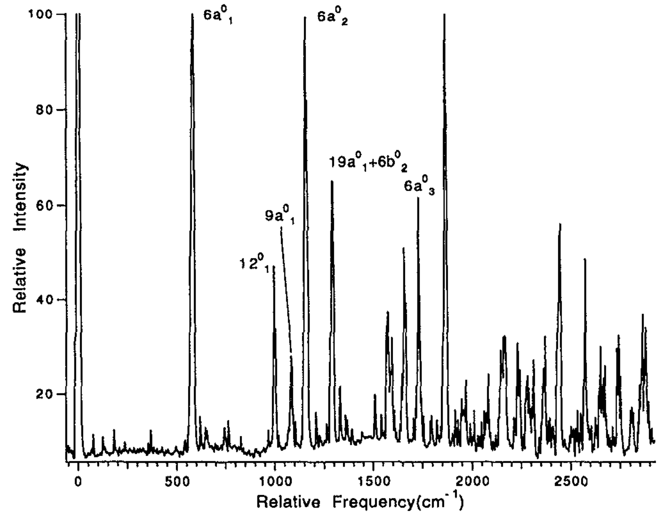

FIG. 4. Dispersed fluoresence spectrum resulting from excitation of the S_1 zero point level of 2-mp taken at a resolution of 20 cm^{-1} FWHM.

tions are collected in Table III together with our tentative assignments for the vibrations. Since much of the vibronic activity involves modes with clear analogs in pyrimidine, we have chosen to retain the vibrational numbering scheme of pyrimidine[11,12] in identifying transitions in 2-mp. The reader should be aware, however, that while these normal modes often retain the same general character they possessed in pyrimidine, methyl substitution can modify these motions, in some cases significantly. In cases where internal rotor designations are not included, $\Delta m = 0$ transitions are to be assumed. Internal rotor designations, such as $(0a_1')$ are always placed in parentheses after the vibrational designations, where the number refers to the internal rotor quantum number "m" followed by its symmetry designation (e.g., a_1') in G_{12}.

As shown in Table III, the infrared transitions with frequencies below 700 cm^{-1} are closely analogous to those of 5-mp obtained by Kartha.[12] The symmetries and assignments of these vibrations are thus carried over from 5-mp to 2-mp. Higher frequency vibrations are closely spaced, making firm assignments difficult. Here the dispersed fluorescence spectra provide some guidance, since only totally symmetric vibrational fundamentals are present in the dispersed fluorescence spectrum.

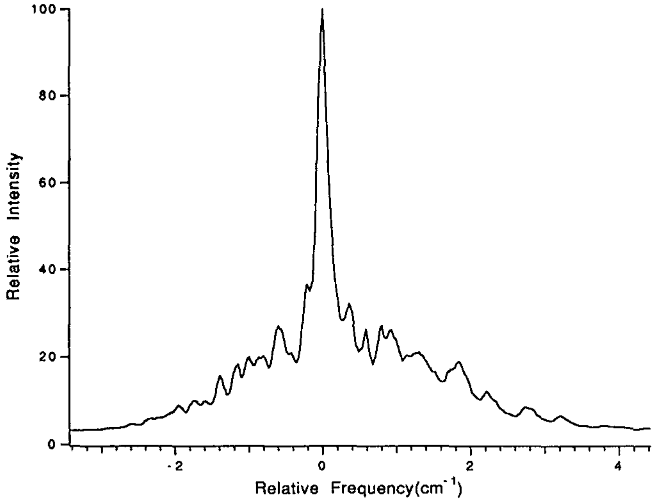

FIG. 3. Fluoresence excitation scan of the rotational band contour of the $S_1 \leftarrow S_0$ origin transition of 2-mp taken at a resolution of 0.08 cm^{-1} FWHM.

TABLE II. Major vibronic transitions in the first 2500 cm^{-1} of the dispersed fluoresence spectrum resulting from pumping the 0_0^0 transition of 2-methylpyrimidine.

Frequency (cm^{-1})[a]	Relative intensity	Assignments
0		0_0^0
583	100	$6a_1^0$
995	47	12_1^0
1082	28	$9a_1^0$
1157	99	$6a_2^0$
1290	65	$19a_1^0 + 6b_2^0$(?)
1573	37	$6a_1^0 12_1^0$
1596	32	?
1657	51	$6a_1^0 9a_1^0$
1729	62	$6a_3^0$
1865	100	$6a_1^0 19a_1^0$
2165	32	$9a_2^0$
2445	56	$6a_2^0 19a_1^0$
2573	49	$19a_2^0$

[a] Frequencies listed are red shifts from the origin which has an absolute frequency of 30 467 cm^{-1}.

TABLE III. Ground state frequencies (cm^{-1}) and symmetry designations of the low-frequency vibrations of 2-mp and 5-mp.

5-mp[a] frequency	Symmetry	2-mp[b] frequency	Assignment
216	a_2''	192	C–CH$_3$ out-of-plane bend (17*b*) + 16*b*
330	a_1''	373	C–CH$_3$ in-plane bend
400	a_2'	395	16*a*, ring torsion
426	a_2''	466	16*b* ring torsion + 17*b*
558	a_1'	576	6*a*
635	a_1''	639	6*b*
728	a_2''	748	4
815	a_1'	810	1
878	···	···	C–H out of plane
884	···	···	C–H out of plane
965	···	980	C–H out of plane
1046	a_1''	994	12
989	a_1'	1050	···
1104	a_1'	1080	9*a* (symmetric C–H inplane bend)
1124	···	1108	···
1163	···	1161	···
1242	a_1'	1271	19*a* (?)
1312	···	1396	···

[a] The frequencies and assignments in 5-mp are taken from Ref. 12.

[b] The frequencies and assignments are based on comparison of our own infrared spectrum of 2-mp with those of 5-mp, using the DFL spectra as a guide to the assignment of totally symmetric vibrations.

Based on these ground state vibrational assignments, the zero-point level dispersed fluorescence spectrum shows activity in many of the same modes that are active in pyrimidine[11] and 5-mp;[6] namely, 6*a*, 12, 9*a*. One notable exception is the complete absence of activity in ν_1 (810 cm^{-1}), consistent with its absence in the excitation spectrum of Fig. 1.

Our assignments of the major vibronic transitions in the excitation spectrum of 2-mp (Fig. 1 and Table I) are both based on analogy with the spectra of pyrimidine and 5-mp and on support provided by dispersed fluorescence scans. The transition at 540 cm^{-1} is clearly the $6a_0^1$ transition. It is split into a Fermi triad, whose close scrutiny will be taken up in the next section. The peaks at 941, 1040, and 1080 cm^{-1} show relative positions and intensities which mirror those in the same region of the spectrum of 5-mp [Fig. 2(b)]. The 1080 cm^{-1} peak is split in a similar manner to $6a_0^1$ and is at the right position to be the $6a_0^2$ overtone. The dispersed fluorescence spectrum of the 941 cm^{-1} peak [Fig. 5(b)] shows some hints of increased activity in the ν_{12} progression (marked by arrows in the figure), while the corresponding spectrum of the 1040 cm^{-1} peak [Fig. 5(c)] shows increased activity in $9a_n$. As a result, we assign the transition 941 cm^{-1} above the origin as 12_0^1 and the 1040 cm^{-1} peak as $9a_0^1$.

B. The Fermi resonance at $6a_0^1$

A close-up scan of the $6a_0^1$ transition [Fig. 6(a)] shows that it is actually composed of three closely spaced transitions. It seems likely that the extra transition(s) result from Fermi resonance of $6a^1$ with dark background states which gain oscillator strength from $6a_0^1$. However, the presence of *three* transitions is hard to reconcile with a simple Fermi resonance with a single dark vibronic level. If one were to ignore the presence of internal rotor levels, then Fermi resonance with a single background vibronic level would lead to two observed transitions rather than three. Even in the presence of internal rotor levels, if the coupling of the $6a^1(0a_1')$ and $6a^1(1e'')$ levels with the background $X^mY^n(0a_1')$ and $X^mY^n(1e'')$ levels is similar, only two transitions would be

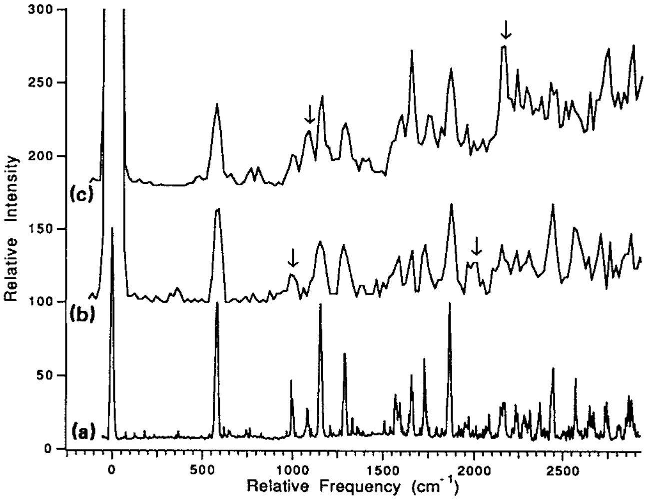

FIG. 5. Dispersed fluoresence spectra resulting from excitation of two levels above the $S_1 \leftarrow S_0$ origin of 2-mp. (a) 0_0^0; (b) 12_0^1; (c) $9a_0^1$. Scans (b) and (c) were taken at a monochromator resolution of 58 cm^{-1} FWHM.

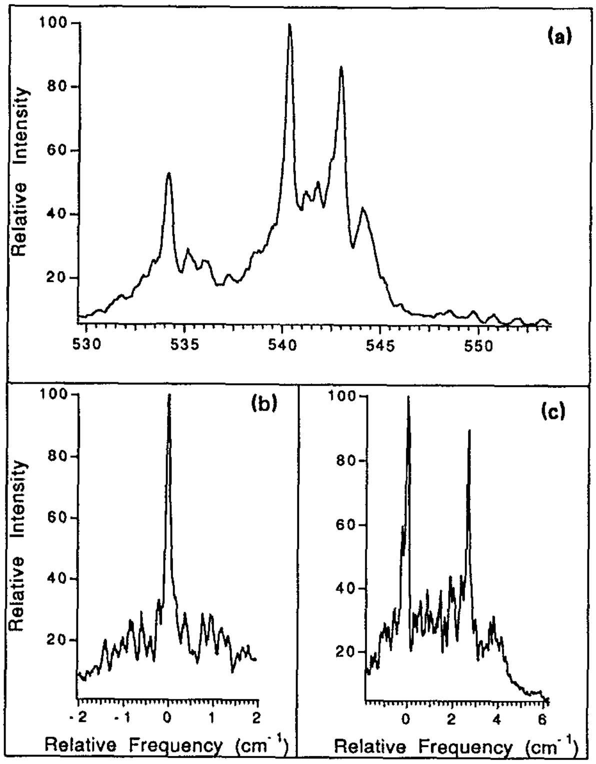

FIG. 6. Fluoresence excitation spectra of the $6a_0^1$ transition of 2-mp. (a) The overview scan at a resolution of 0.3 cm^{-1} FWHM. Etalon scans of the (b) red and (c) middle and blue members of the triplet at a resolution of 0.08 cm^{-1} FWHM.

observed. On the other hand, if the $0a_1' \leftrightarrow 0a_1'$ and $1e'' \leftrightarrow 1e''$ couplings are different, *four* transitions should be observed.

In order to be sure that the observation of three transitions does not arise simply because the fourth transition is not resolved in the spectrum, we have recorded higher resolution etalon scans of the three transitions [Figs. 6(b) and 6(c)]. These show clearly that there are only three distinct Q branches in the spectrum, each with band contours qualitatively similar to the band contour at the origin.

Dispersed fluoresence spectra of the red-shifted, middle, and blue-shifted peaks are shown in Figs. 7(b)–7(d), respectively. The zero point level DFL scan is included in Fig. 7(a) for comparison. These scans provide several pieces of evidence about the nature of the background state involved in the Fermi resonance. First, the peak at 1080 cm^{-1} which is so prominent in the origin dispersed fluorescence scan [Fig. 7(a)] is missing from all three spectra of the Fermi triad. The corresponding transition 1080 cm^{-1} red of resonance in the origin DFL scan is assigned as $6a_2^0$. The absence of a 1080 cm^{-1} transition in Figs. 7(b)–7(d) indicates that all three upper levels have significant $6a^1$ character in the excited state. Large changes in intensity are observed in higher members of the $6a_n^1$ progression as well, consistent with this assignment.

Second, while all three spectra show a resemblance to one another, the DFL spectra of the red- and blue-shifted peaks [Figs. 7(b) and 7(d)] exhibit extra transitions which are not present in the DFL scans of either the origin [Fig. 7(a)] or the middle peak at $6a_0^1$ [Fig. 7(c)]. It appears that the red- and blue-shifted peaks are tied to one another through coupling not present in the middle peak. The most notable of the extra transitions occurs 510 cm^{-1} red of the resonance peak. Similar transitions appear shifted by 510 cm^{-1} from other strong transitions in the spectra of Figs. 7(b) and 7(d). Table III indicates that there is no totally symmetric vibrational fundamental or vibrational combination band which occurs in this frequency range. However, ν_{16b} (466 cm^{-1}) and the internal rotor level $3a_2''$ are both of

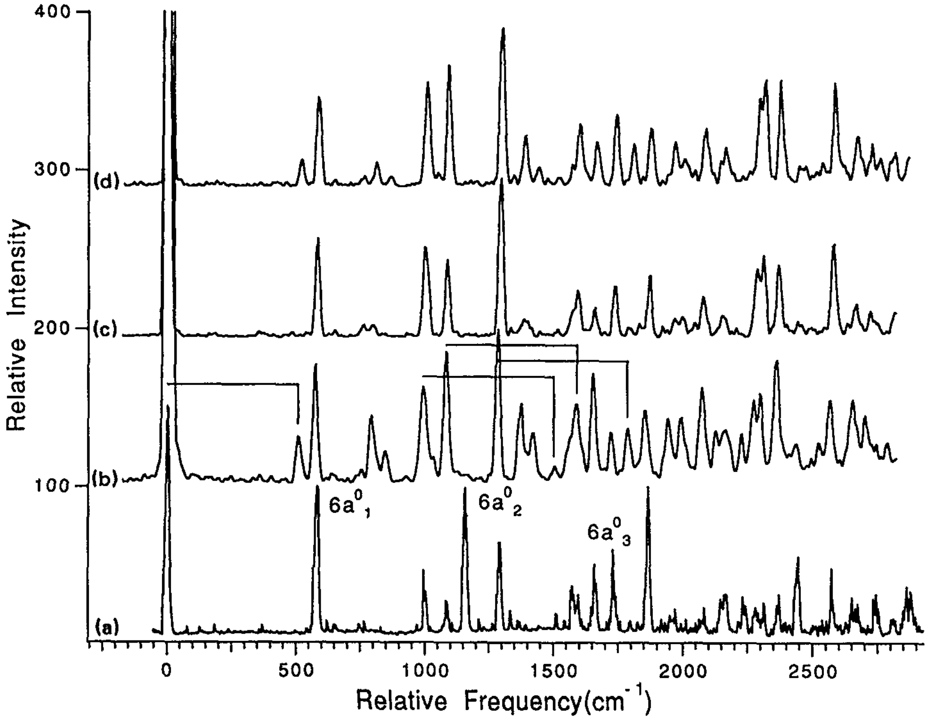

FIG. 7. Dispersed fluoresence spectra resulting from excitation of each of the transitions at $6a_0^1$ compared to that from the origin 0_0^0. (a) 0_0^0; (b) $6a_0^1$ red; (c) $6a_0^1$ middle; (d) $6a_0^1$ blue. Scans (b), (c), and (d) were taken at a monochromator resolution of 23 cm^{-1} FWHM.

a_2'' symmetry so that the $16b^1(3a_2'')$ combination band possesses the necessary a_1' symmetry needed to couple to $6a^1(0a_1')$. Since 2-mp is nearly a free rotor in the S_1 state, the energy of the $3a_2''$ internal rotor level[8] is $E = B\cdot m^2 = (5.47\ \mathrm{cm}^{-1})\cdot 9 = 49\ \mathrm{cm}^{-1}$, predicting a combination band at 515 cm^{-1}, just as is observed. Thus, we assign the 510 cm^{-1} band to the $16b_1^1(3a_2''-3a_2'')$ transition arising from Fermi resonance mixing of the $6a^1(0a_1')$ level with the $16b^1(3a_2'')$ combination band. Its presence in the DFL spectra of the red- and blue-shifted peaks results from the $\Delta v = 0$, $\Delta m = 0$ propensity expected of a nontotally symmetric vibration/free internal rotation combination band.

New transitions in the DFL spectra of the red- and blue-shifted peaks also appear at 790 and 850 cm^{-1} from resonance and as combination bands built on other strong transitions in the spectrum. Their absence in the origin and $6a^1$ middle DFL spectra indicate that they also arise from the $16b^1(3a_2'')$ character of the mixed upper levels. The most likely assignment for the 790 cm^{-1} peak is as the $16b_0^1 4_1^0(3a_2''-3a_2'')$ transition involving another vibrational mode of a_2'' symmetry (ν_4, 748 cm^{-1}), which predicts a peak at $748 + 49 = 797$ cm^{-1}. This transition may have good Franck–Condon factors which are not present in the uncoupled $6a^1(1e'')$ level. The transition at 850 cm^{-1} remains unassigned.

The assignment of the background state involved in the Fermi resonance to the $16b^1(3a_2'')$ vibration/internal rotation combination band also explains the presence of three transitions in the excitation scan. As Fig. 8 indicates, the $16b^1(3a_2'')$ transition is of the correct symmetry to couple only with $6a^1(0a_1')$, but not with $6a^1(1e'')$. Furthermore, the close-lying $16b^1(3a_1'')$ level cannot couple with either $6a^1(0a_1')$ or $6a^1(1e'')$ and so is not involved in the Fermi resonance in any way. The $16b^1(4e')$ level is of the correct symmetry to couple with $6a^1(1e'')$, but the free rotor energy level spacing places $16b^1(4e')$ 32 cm^{-1} above the $6a^1(1e'')$ level, a great enough distance to minimize the coupling between these two states. As a result, the red-shifted and blue-shifted peaks in the excitation scan are transitions to upper states of mixed $16b^1(3a_2'')$ and $6a^1(0a_1')$ character, while the middle peak is a nearly pure $6a_0^1(1e''-1e'')$ transition (Fig. 8).

The simple two-level Fermi resonance between $6a^1(0a_1')$ and $16b^1(3a_2'')$ allows us to determine both the mixing coefficients and the coupling matrix element from the positions and intensities of the red- and blue-shifted transitions in the fluorescence excitation spectrum of Fig. 6(a). The mixed wave functions will be of the form $\alpha|6a^1(0a_1')\rangle + \beta|16b^1(3a_2'')\rangle$ and $\beta|6a^1\rangle - \alpha|16b^1(3a_2'')\rangle$.[13] It is highly unlikely that the $16b_0^1(0a_1'-3a_2'')$ transition will have significant intensity apart from coupling of $16b^1(3a_2'')$ to $6a^1(0a_1')$. Neither the $16b_0^1$ nor $(0a_1'-3a_2'')$ transitions are allowed apart from vibration/internal rotation coupling. Thus, the observed intensities of the red- and blue-shifted peaks reflect directly the fractional $6a^1(0a_1')$ character of the mixed states. The ratio of their intensities is just

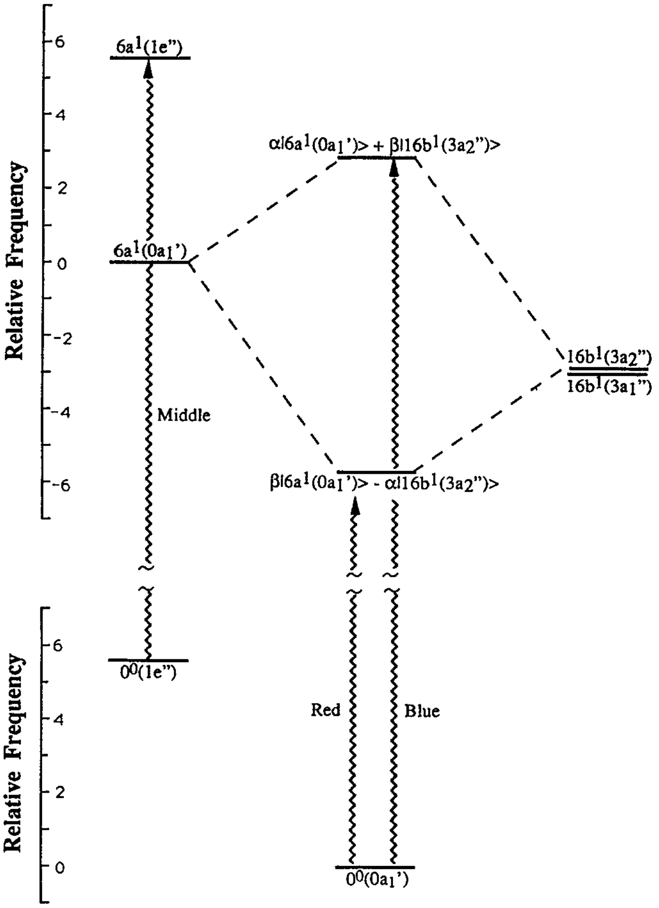

FIG. 8. The energy level diagram depicting the selective coupling of the $6a_0^1(0a_1')$ and $16b^1(3a_2'')$ levels in 2-mp. The energy levels are at their correct energies derived from an analysis of the mixing coefficients ($\alpha = 0.79$, $\beta = 0.61$) and coupling matrix element ($V_{12} = 4.1$ cm^{-1}) given in the text.

$$\frac{I(\text{blue})}{I(\text{red})} = 1.71 = \left(\frac{\alpha}{\beta}\right)^2.$$

Applying normalization leads to $\alpha = 0.79$ and $\beta = 0.61$.

Furthermore, the fact that the $6a^1(1e'')$ level is not involved in the Fermi resonance provides us with a marker for the position of the uncoupled $6a^1(0a_1')$ level. Recall that at the origin (Fig. 3), the $0_0^0(0a_1'-0a_1')$ and $0_0^0(1e''-1e'')$ transitions were unresolved in the spectrum. As a result, the $6a_0^1(1e''-1e'')$ transition occurs at the same position that the $6a_0^1(0a_1'-0a_1')$ transition would occur if it were not Fermi resonance mixed. Taking E_1 and E_2 as the energies of the uncoupled $6a^1(0a_1')$ and $16b^1(3a_2'')$ levels, the energies of the Fermi-coupled levels $E_\pm$ are given by[13]

$$E_\pm = 1/2(E_1 + E_2) \pm 1/2\{(E_1 - E_2)^2 + 4V_{12}^2\}^{1/2},$$

where V_{12} is the $6a^1(0a_1')-16b^1(3a_2'')$ coupling matrix element. Taking our zero of energy as $E_1 = 0$ makes $E_+ = +2.8$ cm^{-1} and $E_- = -5.96$ cm^{-1}. Solving for E_2 and V_{12} yields $E_2 = -3.16$ cm^{-1} and $V_{12} = 4.1$ cm^{-1}. The energy level diagram of Fig. 8 shows the coupled levels at their correct relative energies.

Several comments should be made.

First, despite the obvious similarities in much of the spectroscopy of 2-mp and 5-mp, the $6a^1(0a_1')\leftrightarrow 16b\,^1(3a_2'')$ Fermi resonance is completely absent from the 5-mp spectrum. Its absence is likely the result of a lowering of the ν_{16b} vibrational frequency in 5-mp by comparison to 2-mp. In the ground state of 5-mp, ν_{16b} is 426 cm^{-1} (Table III), 40 cm^{-1} lower than in 2-mp.[12] Since the excited state frequency of 6*a* is nearly identical in the two molecules (532 vs 540 cm^{-1}), a significant lowering of ν_{16b} in 5-mp separates the $16b\,^1(3a_2'')$ and $6a^1(0a_1')$ levels by enough that the Fermi resonance condition is effectively broken.

Second, the Fermi resonance present in 2-mp is unusual and informative since it involves levels which differ both in their vibrational and internal rotor quantum numbers, i.e., it is a consequence of vibration/internal rotation coupling. The Fermi resonance thus provides an explicit example of the new types of mechanisms opened for vibrational state mixing in a molecule following methyl substitution. As we have already stated, the methyl rotor in 2-mp undergoes essentially free internal rotation under the influence of a barrier of only 2 cm^{-1} in the S_1 state. The symmetric position of methyl substitution in 2-mp insures that this barrier is a pure sixfold barrier. As a result, in the undistorted molecule, coupling between internal rotor levels is restricted[14] to levels in which $\Delta m = 0, \pm 6,\ldots$ in order that $\langle m_f|(1+\cos 6\phi)|m_i\rangle \neq 0$. The coupling we observe involves $\Delta m = 3$, in apparent violation of these selection rules. However, ν_{16b} is a nontotally symmetric out-of-plane vibration which distorts 2-mp away from its symmetric equilibrium position. It is this asymmetric distortion of the molecule upon excitation of ν_{16b} which produces a threefold contribution to the internal rotor barrier, giving rise to $\Delta m = 3$ contributions to the observed state mixing.

Third, the magnitude of the $16b\,^1(3a_2'')\leftrightarrow 6a^1(0a_1')$ coupling matrix element is in remarkable agreement with the theoretical estimates of average coupling matrix elements by Moss *et al.*[14] on *p*-fluorotoluene, a molecule which also possesses a nearly freely rotating methyl group [$V_6(S_1) = 34$ cm^{-1}]. The theoretical model advanced by these workers targets van der Waals interactions between the methyl rotor and the ring as the primary source of the barrier to internal rotation and of vibration/internal rotation coupling. 2-mp possesses an even smaller barrier [$V_6(S_1)\sim 2$ cm^{-1}], consistent with the expectation that the nitrogen heteroatoms straddling the methyl group will produce even less steric hindrance than the hydrogen atoms present in *p*-fluorotoluene. Moss, *et al.*[14] estimate average coupling matrix elements between vibration/internal rotation levels which they categorize according to the vibrational quantum number change, showing a steep dropoff as Δv increases. In 2-mp, we have determined an experimental value for the coupling matrix element (4.1 cm^{-1}) in a specific case; namely, $\langle 16b\,^1(3a_2'')|V|6a^1(0a_1')\rangle$ with $\Delta v = 2$ and $\Delta m = 3$. This value is completely consistent with the average coupling matrix elements computed in their model for such a transition $V_{12}\sim 1$ cm^{-1}. This excellent correspondence lends credence to the general physical picture of Moss, *et al.*[14] that van der Waals interactions play a dominant role in vibration/internal rotation coupling, at least in molecules having small internal rotor barriers.

Fourth, the present work offers a good comparison with our earlier observation of a similar Fermi resonance in 4-mp.[6] Though the evidence is less definitive in 4-mp than that presented here for 2-mp, in 4-mp the $6a^1(0a_1')$ level is also perturbed significantly by mixing with the same $16b\,^1(3a_2'')$ vibration/internal rotation level. In that case, however, we could only place a lower bound on the coupling matrix element of $V_{12}\geqslant 17$ cm^{-1}. The much greater coupling observed in 4-mp is the result of a much higher, threefold barrier to internal rotation ($V_3 = 740$ cm^{-1}).[6] This high barrier is almost certainly the result of hyperconjugation effects with the ring. Vibrational excitation in 16*b* must then modulate these interactions, producing large effects on the barrier to internal rotation, leading to the greater observed coupling between the levels in 4-mp.

C. Second-order coupling with background levels at $6a_0^2$

Figure 9(a) presents a close-up fluorescence excitation scan of the next member of the 6*a* progression $6a_0^2$ for comparison with $6a_0^1$ [Fig. 9(b)]. It is obvious from the figure that $6a^2$ is undergoing the same Fermi resonance interaction as $6a^1$, now between $6a^2(0a_1')$ and $6a^1 16b\,^1(3a_2'')$. Both the spacing and relative intensities of the triad are virtually unchanged from $6a_0^1$, indicating that the uncoupled energy levels are at virtually identical positions relative to one another at $6a^1$ and $6a^2$, and that the coupling matrix element to $16b\,^1(3a_2'')$ is also unchanged.

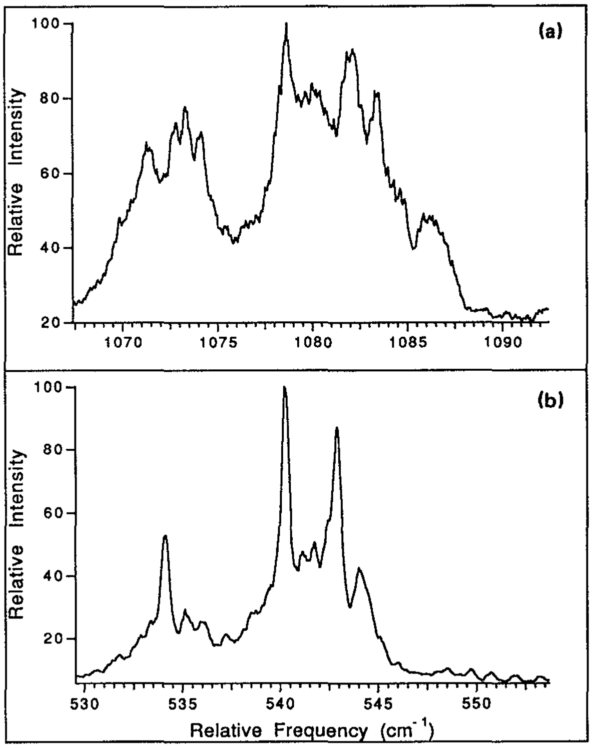

FIG. 9. Fluoresence excitation spectra of 2-mp at (a) $6a_0^1$ and (b) $6a_0^2$ taken at a resolution of 0.3 cm^{-1} FWHM. Note the similarity in the overall contours of the two spectra, indicating that the Fermi resonance present in $6a^1$ [i.e., $6a^1\leftrightarrow 16b\,^1(3a_2'')$] is also present in $6a^2$ [i.e., $6a^2\leftrightarrow 6a^1 16b\,^1(3a_2'')$].

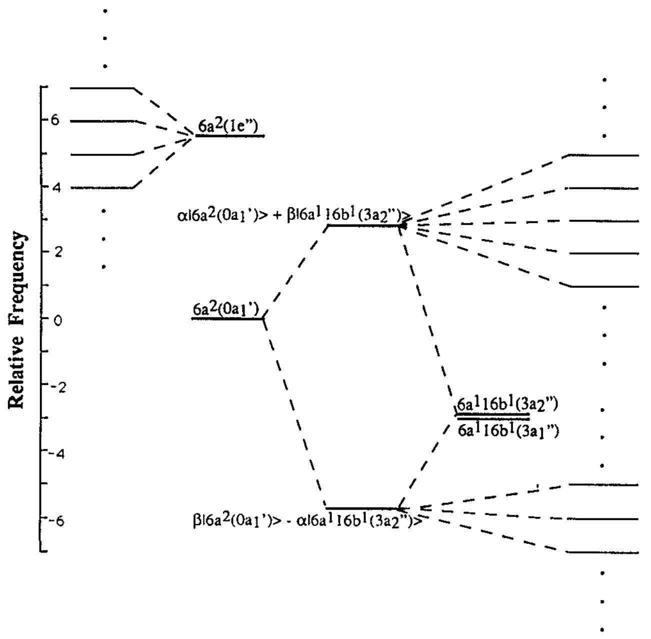

FIG. 10. The energy level diagram depicting the "second-tier" coupling of the $6a^2$ level of 2-mp with the bath of dark vibration/internal rotation states at the same energy. See the text for further explanation.

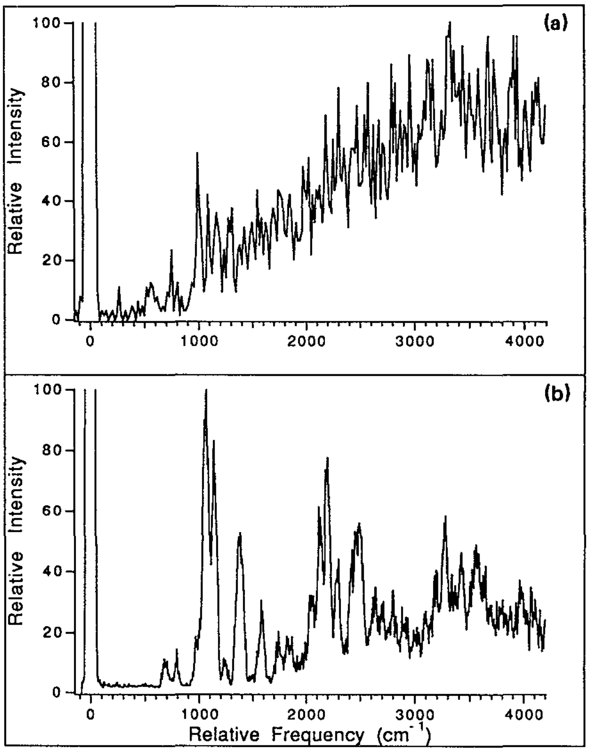

FIG. 11. Dispersed fluoresence spectra resulting from excitation of the $6a_0^2$ transition in (a) 2-mp and (b) pyrimidine. The "second-tier" coupling present in 2-mp at this energy is manifested as a large, unstructured emission in the 2-mp spectrum. See the text for further explanation.

However, the most striking feature of the spectrum of Fig. 9(a) is the strong evidence it provides of weak coupling of the Fermi levels with other background states. Each of the three transitions observed at $6a_0^1$ is broken up into a set of transitions with spacing about 1 cm^{-1} in the spectrum at $6a_0^2$. The $6a^2$ levels are 1080 cm^{-1} above the S_1 origin, twice that of the $6a^1$ levels, resulting in a much higher density of vibration/internal rotation levels at that energy. While the primary coupling of $6a^2(0a_1')$ is still via the Fermi resonance with $6a^1 16b^1(3a_2'')$ with a coupling matrix element of 4 cm^{-1}, the background states present at 1080 cm^{-1} are involved in a weaker, second tier of coupling, as depicted in Fig. 10.

A comparison can be made easily between the observed spacing of background levels and the predicted density of same-symmetry states at that energy. The density of states of the same symmetry as states of interest can be calculated by direct counting, using the known internal rotor energy levels and vibrational frequencies of 2-mp. We have carried out similar calculations previously on 4-mp and 5-mp.[6] At 1080 cm^{-1}, we estimate that the density of same-symmetry levels (which are thereby capable of coupling to the levels carrying the oscillator strength) is about one state/2 cm^{-1}. This is very close to the observed spacing of the second-tier structure in the spectrum of Fig. 9(a). Thus, it appears that a large fraction of the levels of the correct symmetry to couple to the Fermi triad do so. The fact that the oscillator strength from each member of the Fermi triad is spread out over about 5 cm^{-1} means that the second-tier coupling matrix elements have magnitudes of about 1 cm^{-1}.

The DFL spectrum with the laser tuned to the peak of the bands at 1080 cm^{-1} is shown in Fig. 11(a), juxtaposed with the corresponding $6a_0^2$ transition in pyrimidine [Fig. 11(b)] taken at the same monochromator resolution. The comparison highlights once again the much enhanced state mixing which accompanies methyl substitution in a molecule. The $6a^2$ level in pyrimidine is also involved in Fermi resonance mixing,[11] in this case with $6a^1 6b^2$ and $6b^4$. Despite this, its spectrum is composed primarily of well-resolved, structured emission. In the case of 2-mp, the mixing with background levels, even via coupling matrix elements of only 1 cm^{-1}, leads to an almost total washing out of structured emission at this resolution. Estimates of the number of coupled levels N from the ratio of structured to unstructured emission in the DFL spectrum[14] leads to $N = 2.5$, again in keeping with the picture that virtually all states of the correct symmetry are involved in the observed vibrational state mixing.

IV. CONCLUSIONS

Despite its exceedingly low barrier to internal rotation, the presence of the internal rotor levels in 2-mp has a dramatic effect on its photophysics. Vibration/internal rotation coupling is responsible for what might be termed "first-tier" coupling in the $6a_0^n$ progression, where Fermi resonance of the $6a^{n-1} 16b^1(3a_2'')$ level perturbs selectively the $6a^n(0a_1')$ level without disturbing its companion $6a^n(1e'')$ level. The matrix element for the $6a^{n-1} 16b^1(3a_2'')$–$6a^n(0a_1')$ coupling is determined directly from the spectrum to be 4.1 cm^{-1} in $n = 1$. The identical Fermi resonance was observed in our earlier work on the asymmetrically substituted 4-mp.[6] In that case, the much higher barrier to internal rotation provided by hyperconjugation with the ring yields a coupling matrix element at least four times greater than that observed in 2-mp.

Higher members of the $6a_0^n$ progression show, in addition to the first-tier coupling, weaker second-tier coupling to a bath of same-symmetry states with coupling matrix elements of about 1 cm^{-1}. The result of this second-tier coupling is a spreading of the oscillator strength of each first-tier level over about 5 cm^{-1} and an almost total washing out of structured emission in the DFL spectrum. This second-tier coupling is quite indiscriminant in the levels involved in the mixing, as evidenced by the fact that essentially all close-lying levels of the same symmetry appear to be involved. In 5-mp, which lacks the Fermi resonance interaction of 2-mp and 4-mp, this weaker coupling was also evident in levels ~ 1000 cm^{-1} above the origin, suggesting that this weaker coupling is present as a more general feature of state mixing in molecules containing methyl rotors.

ACKNOWLEDGMENTS

Acknowledgement is made to the Donors of the Petroleum Research Fund, administered by the American Chemical Society, for their support of this research. T.S.Z. also thanks the Sloan Foundation for an Alfred P. Sloan Research Fellowship. We also acknowledge the help of Fred Ensminger in recording the infrared spectra of 2-mp.

[1] M. Ito, T. Ebata, and N. Mikami, Annu. Rev. Phys. Chem. **39**, 123 (1988), and references therein.

[2] L. H. Spangler and D. W. Pratt, J. Chem. Phys. **84**, 4789 (1986); X.-Q. Tan, W. A. Majewski, D. F. Plusquellic, and D. W. Pratt, *ibid.* **94**, 7721 (1991); A. E. Dorigo. D. W. Pratt, and K. N. Houk, J. Am. Chem. Soc. **109**, 6591 (1987); J. L. Tomer, S. Yamanuchi, and D. W. Pratt, Chem. Phys. Lett. **175**, 30 (1990).

[3] P. J. Breen, J. A. Warren, E. R. Bernstein, and J. I. Seeman, J. Am. Chem. Soc. **109**, 3453 (1987); P. J. Breen, J. A. Warren, E. R. Bernstein, and J. I. Seeman, J. Chem. Phys. **87**, 1917 (1987).

[4] G. A. Bickel, G. W. Leach, D. R. Demmer, J. W. Hager, and S. C. Wallace, J. Chem. Phys. **88**, 1 (1988).

[5] L. H. Spangler, W. B. Bosma, R. D. van Zee, and T. S. Zwier, J. Chem. Phys. **88**, 6768 (1988).

[6] R. E. Bandy, J. Nash, and T. S. Zwier, J. Chem. Phys. **95**, 2137 (1991).

[7] P. R. Bunker, *Molecular Symmetry and Spectroscopy* (Academic, New York, 1979), p. 388.

[8] W. Caminati, G. Cazzoli, and D. Troiano, Chem. Phys. Lett. **43**, 65 (1976).

[9] L. H. Spangler, R. van Zee, and T. S. Zwier, J. Phys. Chem. **91**, 2782 (1987).

[10] R. G. Pews, Heterocycles **27**, 1867 (1988).

[11] A. E. W. Knight, C. M. Lawburgh, and C. S. Parmenter, J. Chem. Phys. **63**, 4336 (1975).

[12] S. B. Kartha, Spectrochimica Acta Part A **38**, 859 (1982).

[13] P. W. Atkins, *Molecular Quantum Mechanics*, 2nd ed. (Oxford, New York, 1983), p. 172.

[14] D. B. Moss, C. S. Parmenter, and G. E. Ewing, J. Chem. Phys. **86**, 51 (1987).